MAJOR ARTICLE

Murine Model to Study the Invasion and Survival of *Mycobacterium tuberculosis* in the Central Nervous System

Nicholas A. Be,[1] Gyanu Lamichhane,[1] Jacques Grosset,[1] Sandeep Tyagi,[1] Qi-Jian Cheng,[1] Kwang Sik Kim,[2] William R. Bishai,[1] and Sanjay K. Jain[1,2]

[1]Center for Tuberculosis Research and [2]Pediatric Infectious Diseases, Johns Hopkins University School of Medicine, Baltimore, Maryland

Background. Tuberculosis of the central nervous system (CNS) is a serious, often fatal disease primarily affecting young children. It develops after hematogenous dissemination and subsequent invasion of the CNS by *Mycobacterium tuberculosis*. The microbial determinants involved in CNS disease are poorly characterized.

Methods. Hematogenously disseminated *M. tuberculosis* infection was simulated in BALB/c mice by intravenous challenge. Bacteria were recovered using standard culture techniques. Host immune response to *M. tuberculosis* infection was assessed by histopathological and cytokine profile analysis. By means of a pooled infection with genotypically defined *M. tuberculosis* mutants, bacterial genes required for invasion or survival were determined in the CNS and lung tissue.

Results. *M. tuberculosis* were detected in whole mouse brains as early as 1 day after intravenous infection and at all time points assessed thereafter. No significant immune response was elicited in the infected brain tissue, compared with extensive inflammation in the infected lung tissue at the same time point. We identified mutants for 5 *M. tuberculosis* genes (*Rv0311, Rv0805, Rv0931c, Rv0986,* and *MT3280*) with CNS-specific phenotypes, absent in lung tissue.

Conclusions. We have identified CNS-specific *M. tuberculosis* genes involved in the pathogenesis of tuberculosis. Further characterization of these genes will help in understanding the microbial pathogenesis of CNS tuberculosis.

Central nervous system (CNS) tuberculosis is considered to be the most severe extrapulmonary form of the disease, and it predominantly affects young children. The clinical symptoms related to CNS tuberculosis are largely induced by infarction through vasculitis [1]. Mortality, even with rigorous treatment, has been shown to be >16% [1]. Furthermore, of those who survive, ~27% develop severe neurological impairments [2]. Coinfection with HIV increases the risk of the development of CNS tuberculosis several times and also leads to a much higher case-fatality rate [3, 4]. In addition, multidrug-resistant CNS tuberculosis is formidable to treat and results in an outcome much worse than in the case of susceptible organisms [5]. Because severe sequelae are observed even when CNS tuberculosis is treated effectively, our goal is to develop preventive strategies for this disease.

Under normal physiological conditions, the CNS is conditionally isolated from the systemic circulation by the blood-brain barrier (BBB). Transcellular movement is also limited both by reduced pinocytosis and the absence of endothelial fenestrae [6]. Current concepts of how CNS tuberculosis develops are based on studies published in 1933 [7]. These studies suggest that *Mycobacterium tuberculosis* deposits in the brain parenchyma and meninges during hematogenous dissemination. Tuberculomas develop around bacilli that have been deposited in the parenchyma and the meninges. Much later, physical rupture of these tuberculomas causes direct dissemination of bacilli into the cerebrospinal fluid (CSF), leading to tuberculous meningitis [7].

Received 2 October 2007; accepted 7 December 2007; electronically published 27 October 2008.

Potential conflicts of interest: none reported.

Presented in part: 44th Annual Meeting of the Infectious Diseases Society of America, Toronto, 12–15 October 2006 (poster 313); Tuberculosis: From Lab Research to Field Trials (C6), Keystone Symposia, Vancouver, British Columbia, 20–25 March 2007 (poster 125).

Financial support: National Institutes of Health (grants and contracts AI36973, AI37856, AI43846, and N01 AI30036); Center for AIDS Research Pilot Developmental Program, Johns Hopkins.

Reprints or correspondence: Dr. Sanjay Jain, Center for Tuberculosis Research, 1550 Orleans St., Baltimore, MD 21287 (sjain5@jhmi.edu).

The Journal of Infectious Diseases 2008; 198:1520–8

0022-1899/2008/19810-0014$15.00
DOI: 10.1086/592447

Previously, other investigators have described mouse and rabbit models of tuberculosis meningitis after intracisternal inoculation of *M. tuberculosis* directly into the CSF [8, 9]. In humans, however, CNS tuberculosis (and subsequent meningitis) is the result of traversal of *M. tuberculosis* from blood to the CNS. We have previously shown that *M. tuberculosis* can invade and traverse an in vitro model of the human BBB [10]. Furthermore, intravenous inoculation of free *M. tuberculosis* into guinea pigs and rabbits has been shown to produce CNS invasion, as evidenced by the formation of tuberculomas in their brain parenchyma [7, 11]. We therefore developed a murine model to study the invasion of the CNS by *M. tuberculosis* and identify mycobacterial genes involved in the pathogenesis of CNS tuberculosis. Hematogenously disseminated disease, as seen in humans and frequently associated with CNS tuberculosis [5, 12], was simulated using high-dose intravenous challenge.

METHODS

M. tuberculosis *strains and media.* *M. tuberculosis* H37Rv, *M. tuberculosis* CDC 1551, and genotypically defined *M. tuberculosis* CDC 1551 transposon (Tn) mutants, available through the Tuberculosis Animal Research and Gene Evaluation Taskforce [13], were grown in plastic roller bottles or as shaken cultures in plastic tubes at 37°C in Middlebrook 7H9 liquid broth (Difco Laboratories) supplemented with oleic acid albumin dextrose catalase (OADC; Becton Dickinson), 0.5% glycerol, and 0.05% Tween 80. A pool of 28 mutants was randomly selected, with the exception of JHU0986–468 and JHU0987–1595, which were added because of their possible role in CNS infection [10]. Only mutants with in vitro growth similar to that of wild type and with Tn insertions in the upstream regions (as defined elsewhere [14]) were used for the study. From each inoculum, 100 μL was plated to determine the colony-forming unit counts. *M. tuberculosis* H37Rv and CDC 1551 were plated onto Middlebrook 7H11 selective plates (Becton Dickinson), and the Tn mutants were plated onto Middlebrook 7H10 medium (Difco Laboratories) supplemented with OADC, 50 μg/mL cycloheximide (Sigma), and 25 μg/mL kanamycin (Sigma).

Animal infection. All protocols were approved by the Johns Hopkins Animal Care and Use Committee, and 5–6-week-old female BALB/c mice were used for all experiments. For infection with wild-type strains, *M. tuberculosis* were grown to mid-log phase and then diluted to an optical density (OD) at 600 nm of 0.1 in PBS. For infection by Tn mutants, each mutant was grown individually to mid-log phase, and its OD_{600} equalized. Mutants were then added to a pool, using dilutions such that equal proportions of each mutant would be present in the pooled suspension. The pool was then diluted to an OD_{600} of 0.1 in PBS, and 200 μL of either the wild-type strains or the mutant suspension was injected into each mouse intravenously via the tail vein. At the specified time points after infection, mice were anesthetized with isoflurane (Henry Schein), their chest cavities were opened, and blood was obtained via intracardiac puncture under direct visualization. Lungs and brains were obtained and kept in 2.5 mL of PBS overnight. Organs were homogenized and plated on the corresponding media described above.

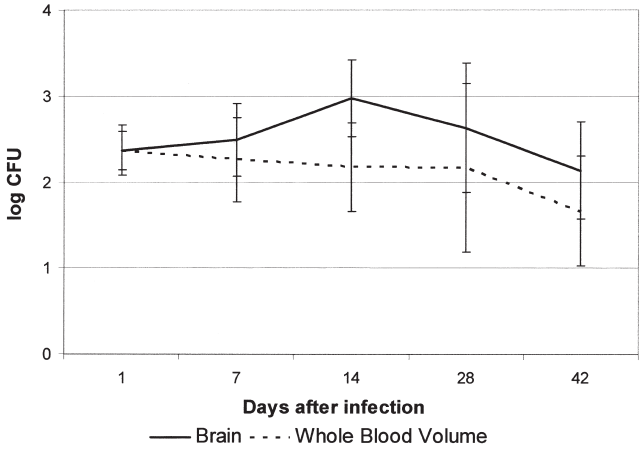

Figure 1. *Mycobacterium tuberculosis* invasion of the central nervous system after intravenous infection. Female BALB/c mice were infected intravenously with 1.01×10^6 cfu of *M. tuberculosis* per mouse. Organs were harvested and homogenized on days 1, 7, 14, 28, and 42 after infection. Log_{10} colony-forming unit counts are shown for the brain *(solid line)* and the blood extrapolated to the whole-blood volume of the mouse *(dashed line).* Note that colony-forming unit counts in the brain are, on average, greater than those present in the whole-blood volume of the mouse, indicating that bacteria in the brain are not due to contamination from the blood.

M. tuberculosis *invasion of CNS after intravenous infection.* Each mouse was inoculated with 200 μL of *M. tuberculosis* CDC 1551 suspension intravenously via tail vein injection. Mice were killed 1, 14, 28, or 42 days after infection, and their organs were harvested and plated. Blood from the same mouse was also cultured at each time point. Colony-forming unit counts for the blood were extrapolated to the expected whole-blood volume of the mouse [15, 16]. At least 3 mice were used at each time point. A fourth mouse was used at each time point for gross pathological and histopathological examination.

***Cytokine and chemokine profile of mouse brain and lung tissues after infection with* M. tuberculosis.** Each mouse was inoculated with 200 μL of *M. tuberculosis* H37Rv suspension intravenously via tail vein injection. At 1, 7, 14, or 28 days after infection, mice were killed, and their organs were harvested and plated. Uninfected control mice were killed on day 1. Parts of the organ homogenates were also used for colony-forming unit counts. The remaining organ homogenates were immediately frozen at −80°C. At a later time, cytokine and chemokine levels were quantified in organ homogenate supernatants using commercially available ELISA kits (R&D DuoSet or Mabtech), in

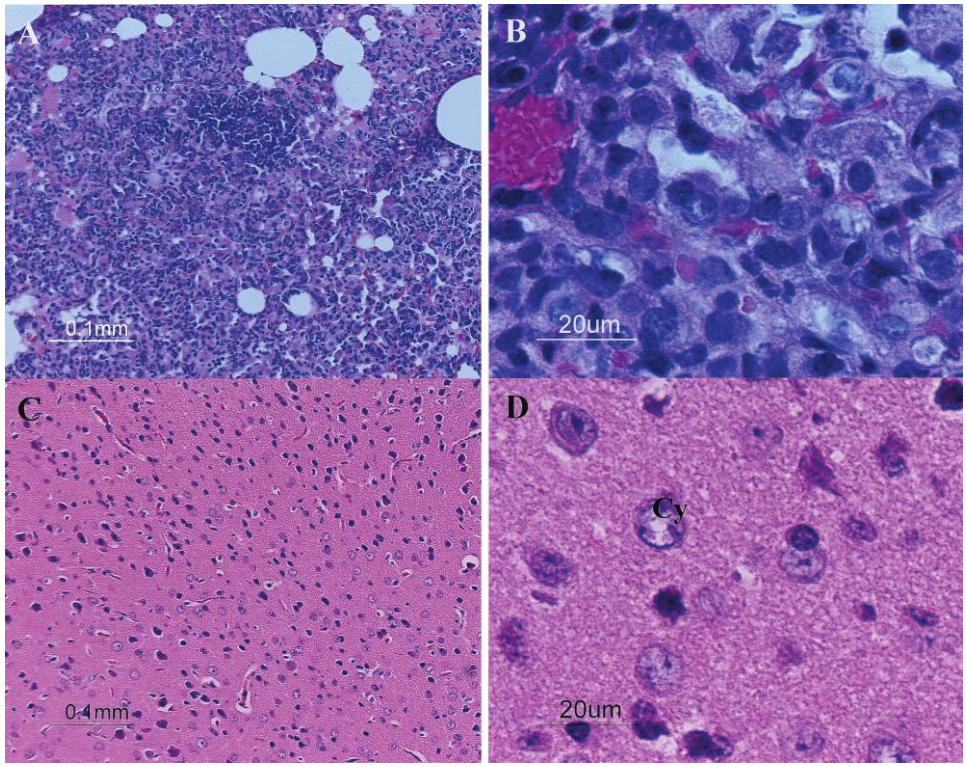

Figure 2. Histopathology in hematoxylin-eosin–stained mouse brain and lung tissues obtained on day 42 after intravenous *Mycobacterium tuberculosis* infection. Lung tissue at ×10 *(A)* and ×60 *(B)* magnification shows extensive inflammation and tissue destruction with numerous inflammatory cells seen throughout the alveoli. Brain tissue at ×10 *(A)* and ×60 *(B)* magnification shows darkly stained nuclei in the cytons (Cy) of the neurons. No inflammatory cells or tissue destruction is observed.

accordance with the manufacturer's suggestions. Three mice were used for each time point in each experiment, with ELISA analysis for each mouse performed in triplicate.

M. tuberculosis *genes involved in invasion or survival in the CNS.* Each mouse was inoculated with 200 μL of the *M. tuberculosis* Tn pool suspension intravenously via tail vein injection. At 1, 14, or 49 days after infection, mice were killed, and their organs were harvested and plated. At each time point, colonies from the plates were scraped and pooled, and genomic DNA was prepared using standard methods [17]. Five mice were used at each time point. Mutant-specific primer sets using Tn and gene-specific primers were designed to amplify 150–200-bp DNA fragments. These primer sets were tested using conventional polymerase chain reaction (PCR), and all were successful in amplifying the correct-sized fragment. Mutant-specific real-time PCR was performed using iCycler iQ (version 3.1.7050; Bio-Rad) at least in triplicate. The cycle threshold for genomic DNA from a given tissue or time point (output pool) was compared with another tissue or earlier time point (input pool), using equal amounts of input and output pool genomic DNA. To further ensure that equal genomic equivalents were used for each comparison, a set of primers that amplify *M. tuberculosis*–specific but mutant independent DNA sequence (gene fragment from *Rv0986,* undisrupted by the Tn insertion) was used as a control for each comparison. There was no significant difference between cycle thresholds for the input and output pool controls in all comparisons made. Attenuation for each mutant was expressed as the ratio of mutants present in the input pool compared with the output pool. JHU0987–1595 was removed from further analysis owing to poor organ implantation on day 1. Mutants were considered attenuated if they had attenuation ratios in the top quartile of the comparison and significantly greater than those for the genomic control ($P < .05$). Mutants identified to have CNS-specific phenotypes were also evaluated in the in vitro human BBB model in triplicate and compared with an intergenic negative control Tn mutant (Tn insertion at base position 921350, between annotated genes *NT02MT0849* and *Rv0829*) [10].

Statistical analysis. Statistical comparison between groups was performed using the *t* test and Microsoft Excel software (2003).

RESULTS

M. tuberculosis *invasion of the CNS after intravenous infection.* Each mouse was inoculated with $1.01 \times 10^6 \pm 3.5 \times 10^5$ bacteria via tail vein injection. *M. tuberculosis* colonies were successfully recovered from whole-brain tissue at all

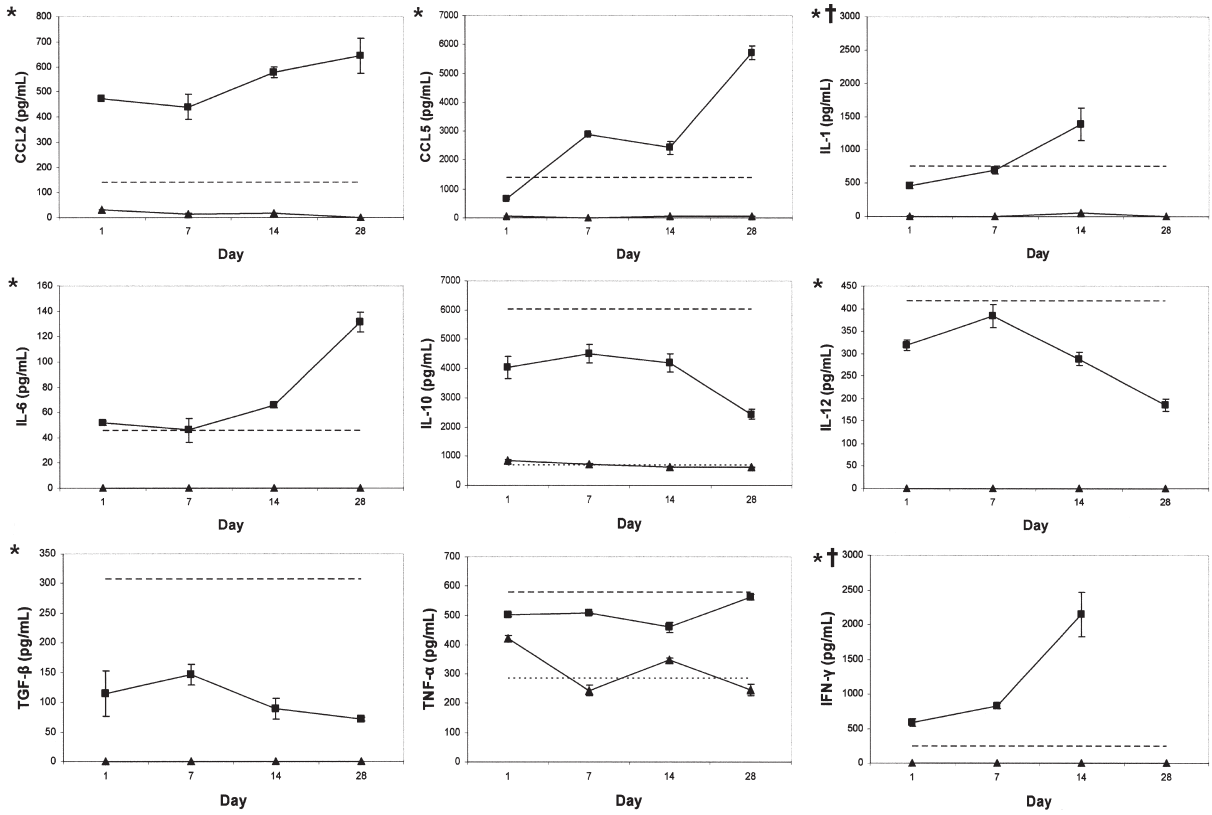

Figure 3. Cytokine and chemokine profile in brain and lung tissues of mice infected with *Mycobacterium tuberculosis*. Levels of cytokines and chemokines in *M. tuberculosis*–infected brain *(black triangles)* and lung *(black squares)* tissue were compared at each time point (days 1, 7, 14, and 28) after intravenous infection. Baseline cytokine and chemokine levels for uninfected mice are indicated for brain *(dotted line)* and lung *(dashed line)* tissues, respectively. For each cytokine or chemokine, levels were significantly lower in the brain than in lung tissue at each time point ($P < .044$). After infection, there was a trend toward progressively increasing levels of CCL2, CCL5, interleukin (IL)–1β, IL-6, and interferon (IFN)–γ in lung tissue over time. Conversely, there was a trend toward progressively reduced levels of IL-10, IL-12, and transforming growth factor (TGF)–β in the lungs after infection. Asterisks (*) indicate that levels of CCL2, CCL5, IL-1β, IL-6, IL-12, IFN-γ, and TGF-β in the brains of uninfected controls were below the limit of detection and were thus omitted from the indicated plots; daggers (†) indicate that levels of IL-1β and IFN-γ in infected lungs were above the limit of detection on day 28 and were thus omitted. TNF, tumor necrosis factor.

time points (days 1, 14, 28, and 42) after infection. Brain counts were $3.40 \times 10^2 \pm 2.53 \times 10^2$ cfu on day 1 and peaked on day 14 ($1.92 \times 10^3 \pm 1.41 \times 10^3$ cfu). As shown in figure 1, on average significantly higher numbers of *M. tuberculosis* were found in the brain than in the whole-blood volume in the mouse, indicating that colony-forming unit counts from the brain were not due to contamination from the blood ($P < .02$). Furthermore, gross pathological examination of the brain did not show any granulomas or infectious lesions in the brain at all time points observed. However, the lungs from the same mice had several lesions at all time points after 14 days of infection. On histopathological examination, while the lung tissue exhibited extensive cellular infiltration and inflammation, the brain tissue lacked such an immune response at all time points observed (figure 2).

***Cytokine and chemokine profile of mouse brain and lung tissues after infection with* M. tuberculosis.** Because the brain and lung tissues are characterized by distinct microenvironments, levels of cytokines and chemokines in *M. tuberculosis*–infected brain and lung tissue were compared at each time point (days 1, 7, 14, and 28) after intravenous infection. Uninfected mice were used as controls. Brain colony-forming unit counts were comparable to the counts from the prior wild-type infection. Day 1 counts were $4.01 \times 10^2 \pm 2.57 \times 10^2$ cfu. As shown in figure 3, for each cytokine or chemokine levels were significantly lower in the brain compared with lung tissue at each time point ($P < .05$). Levels for interleukin (IL)–1β, and interferon (IFN)–γ were above the limit of detection on day 28 in the lung tissue and are therefore not shown.

M. tuberculosis *genes involved in invasion or survival in the CNS.* It was hypothesized that, because of the differing microenvironments in the brain and lung tissues, there may be *M. tuberculosis* genes specifically involved in the invasion of and survival in brain tissue, distinct from those in the lungs. Each mouse was intravenously injected with $1.66 \times 10^6 \pm 3.92 \times 10^4$ cfu of a pool comprising equal numbers of each of the 28 genotypically defined *M. tuberculosis* mutants (table 1). On days 1, 14, and 49 after infection, the relative numbers of

Table 1. *Mycobacterium tuberculosis* transposon (Tn) mutants tested in the murine central nervous system invasion model.

JHU no.	Rv no.	MT no.	Function/probable function	Gene size, bp	Point of Tn insertion
JHU3280A-78	. . .	3280	Hypothetical protein	186	78
JHU3428A-203	. . .	3428	Transcriptional regulator	1146	203
JHU0160c-1219	0160c	0169	Proline-glutamate family protein	1509	1219
JHU0311–108	0311	0324	Hypothetical protein	1230	108
JHU0470A-188	0470A	0487	Hypothetical protein	441	188
JHU0488–168	0488	0507	Transporter, LysE/YggA family	606	168
JHU0518–491	0518	0539	Hypothetical protein	696	491
JHU0727c-146	0727c	0752	AraD/FucA family	657	146
JHU0805–6	0805	0825	Phosphodiesterase	957	6
JHU0931c-1166	0931c	0958	Serine-threonine protein kinase	1995	1166
JHU0986–468	0986	1014	ABC transporter	747	468
JHU0987–1595	0987	1015	ABC transporter	2568	1595
JHU1493–184	1493	1540	Methylmalonyl-CoA mutase	2253	184
JHU1558A-302	1510	1558	Hypothetical protein	519	302
JHU1529–73	1529	1580	Acyl-CoA synthase	1755	73
JHU1777–295	1777	1827	P450 heme-thiolate protein	1305	295
JHU1811–488	1811	1859	Mg^{2+} transport protein	705	488
JHU1858–616	1858	1906	ABC transporter	738	616
JHU1887–646	1887	1935	Hypothetical protein	1158	646
JHU1936–15	1936	1986	Luciferase-related protein	1110	15
JHU2058c-165	2058c	2118	Ribosomal protein L28	237	165
JHU2067c-923	2067c	2127	Hypothetical protein	1224	923
JHU2292c-94	2292c	2349	Hypothetical protein	225	94
JHU2476c-92	2476c	2551	Hypothetical protein	4875	92
JHU2545–149	2545	2621	Hypothetical protein	279	149
JHU2778c-270	2778c	2848	Hypothetical protein	471	270
JHU3250c-27	3250c	3348	Rubredoxin	183	27
JHU3424c-26	3424c	3532.2	Hypothetical protein	362	26

NOTE. ABC, ATP-binding cassette.

each mutant in various tissues were evaluated by quantitative PCR using mutant-specific primer sets. Brain colony-forming unit counts were comparable to the counts from the prior wild-type infections. Day 1 counts were $2.45 \times 10^3 \pm 1.35 \times 10^3$ cfu. Five mutants (JHU0311–108, JHU0805–6, JHU0931c-1166, JHU0986–468, and JHU3280A-78) were found to be significantly attenuated in brain tissue compared with the lungs on day 1 and/or day 49 ($P < .03$) (table 2).

To further determine whether attenuation of these mutants was due to a defect in their ability to invade and/or survive in brain tissue, several other comparisons were made. To identify mutants defective in their ability to invade the brain from the bloodstream, attenuation of mutants on day 1 in brain tissue was compared with findings in blood obtained just after infection. Mutants JHU0805–6 and JHU0986–468 were observed to be significantly attenuated, suggesting a role for *Rv0805* and *Rv0986* in invasion of the CNS ($P < .01$). JHU3280A-78 was also attenuated (table 3), but this result was not statistically significant ($P = .10$). Attenuation of mutants on day 49 compared with day 1 in the brain was used to identify mutants defective in their ability to survive in brain tissue. JHU0311–108, JHU0805–6, and JHU931c-1166 were found to be significantly attenuated, suggesting a role for *Rv0311, Rv0805,* and *Rv0931c* in survival in the CNS ($P < .02$). Finally, attenuation of mutants in the lungs on day 49 was compared with that on day 1 to identify mutants defective in their ability to survive in lung tissue. Interestingly, although other mutants were found to be attenuated for survival in lung tissue (table 3), none of the 5 mutants (JHU0311–108, JHU0805–6, JHU0931c-1166, JHU0986–468, and JHU3280A-78) was observed to be attenuated in its ability to survive in lung tissue. This suggests a CNS-specific role for *M. tuberculosis* genes *Rv0311, Rv0805, Rv0931c, Rv0986,* and *MT3280*. Results of analyses comparing attenuation on day 14 (data not shown) were consistent with the results described above. Furthermore, single infections in an in vitro model of the BBB confirmed a defective invasion/survival phenotype for these 5 CNS-specific mutants compared with the negative control Tn mutant ($P < .01$) (figure 4).

Table 2. ***Mycobacterium tuberculosis*** **genes involved in the invasion of or survival in the central nervous system.**

JHU no.	Rv no.	MT no.	ORF description	Fold attenuation for invasion of and survival in brain tissue compared with lung tissue		Fold attenuation for	
				Day 1	Day 49	Invasion of brain tissue	Survival in brain tissue
JHU0311–108	0311	0324	Hypothetical protein	. . .	17.70	. . .	20.12
JHU0805–6	0805	0825	Phosphodiesterase	. . .	17.08	24.66	23.66
JHU0931c-1166	0931c	0958	Serine-threonine protein kinase	. . .	431.25	. . .	1305.93
JHU0986–468	0986	1014	ABC transporter	17.51	35.03	1.52	. . .
JHU3280A-78	. . .	3280	Hypothetical protein	. . .	5.75	. . .	. . .

NOTE. Shown is attenuation as measured by quantitative polymerase chain reaction analysis for the transposon mutants attenuated in the brain compared with lung tissues after intravenous challenge of mice with a mutant pool. Fold attenuation for each mutant is expressed as the ratio of mutants present in the input pool compared with the output pool. As shown, all 5 mutants were found to be highly attenuated (>5-fold) in the brain compared with lung tissues on day 1 or 49 ($P < .03$). To identify mutants defective in their ability to invade the brain from the bloodstream, attenuation of mutants on day 1 in brain tissue was compared with findings in the bloodstream. JHU0805–6 and JHU0986–468 were found to be significantly attenuated (>1.5-fold) in their ability to invade brain tissue from the bloodstream on day 1 ($P < .01$). Attenuation of mutants on day 49 compared with day 1 in the brain was used to identify mutants defective in their ability to survive in brain tissue. As shown, JHU0311–108, JHU0805–6, and JHU931c-1166 were found to be significantly attenuated (>20-fold) in their ability to survive in brain tissue ($P < .02$). Ellipses indicate mutants not found to be significantly attenuated in the tissue at the time point evaluated. ABC, ATP-binding cassette; ORF, open reading frame.

DISCUSSION

The model described in the present study is distinct from previous models employing intracisternal inoculation of *M. tuberculosis* [8, 9]. We wanted to study invasion of the CNS by *M. tuberculosis* and simulate natural human CNS tuberculosis as part of hematogenously disseminated disease. Furthermore, because studies by Rich and McCordock [7] and others [11] demonstrated that intravenous inoculation of *M. tuberculosis* in experimental animals resulted in several lesions in the brain parenchyma but did not lead to meningitis, we opted to detect *M. tuberculosis* in whole-brain tissue, including the parenchyma, instead of just the CSF. Indeed, we were successful in detecting *M. tuberculosis* in brain tissue at each time point after intravenous infection. Furthermore, the mean colony-forming unit counts in brain tissue were higher than those in the whole-blood volume of the mouse, precluding the possibility of brain tissue contamination by extraneous bacteria from the blood. However, we are unable to state with certainty whether, after invading the CNS, *M. tuberculosis* resides primarily within the parenchyma of the brain, the vessel wall, or the endothelial cells lining the microvasculature. Significant vasculitis associated with CNS tuberculosis [1] and human endothelial cell invasion observed in vitro [10] suggest that *M. tuberculosis* resides, at least initially, in the endothelial cells lining the microvasculature.

Table 3. Mutants attenuated for invasion and/or survival in the brain.

The table is available in its entirety in the online edition of the *Journal of Infectious Diseases*.

Gross and histopathological analysis of the infected tissue showed no lesions or host inflammatory cells within the brain tissue. This observation was in stark contrast to extensive lymphocytic and granulocytic infiltration in lung tissue in the same animal at the same time point. Consistent with our histopathological analysis, cytokine and chemokine levels were significantly lower in the brain compared with lung tissue obtained from the same animal at each time point. Tumor necrosis factor–α was the only cytokine observed at appreciable levels in the brain, with levels similar to those in uninfected controls. Levels of CCL2 and CCL5, which target monocytes, macrophages, and activated T cells [18], and IL-1β, IL-6, and IFN-γ, which cause leukocyte activation [19], were elevated in lung tissue but were significantly lower in brain tissue, consistent with a lack of recruitment of inflammatory cells in brain tissue. Lack of inflammation in the brain is consistent with clinical data and findings in other experimental models [20–22]. The brain parenchyma is an immunologically "privileged" site, perhaps owing to the poor antigen-presenting capability of microglia (the predominant antigen-presenting cells in the brain parenchyma) [23]. Heat-killed mycobacteria injected into the brain are sequestered on the "brain side" of the BBB for months. Formation of focal lesions occurs later after recognition of the mycobacteria by the immune system outside the CNS [24]. Our model may therefore provide insights into the pathogenesis of delayed paradoxical enlargement of intracranial tuberculomas during antituberculous therapy, which may arise after mycobacterial destruction and enhanced immune responses elicited by effective therapy [22].

Our analysis did not permit data collection several months after infection, because of the death of mice 7–8 weeks after the

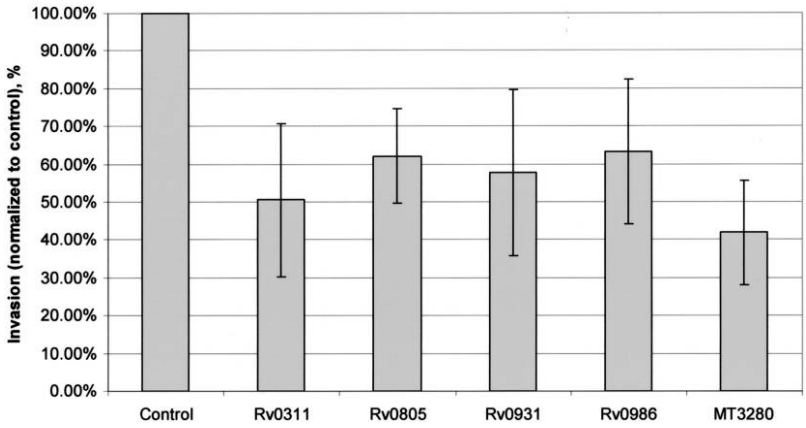

Figure 4. Invasion or survival for the 5 central nervous system (CNS)–specific *Mycobacterium tuberculosis* mutants in the in vitro human blood-brain barrier (BBB) model. Mutants identified to have CNS-specific phenotypes were also evaluated in the in vitro human BBB model in triplicate and compared with an intergenic negative control transposon (Tn) mutant (Tn insertion at base position 921350, between annotated genes *NT02MT0849* and *Rv0829*) that does not have an invasion/survival defect. The invasion or survival rate of mutants for genes *Rv0311, Rv0805, Rv0931c, Rv0986,* and *MT3280* was 50.6% ($P = .002$), 62.1% ($P = .001$), 57.7% ($P = .006$), 63.3% ($P = .006$), and 41.9% ($P < .001$), respectively, compared with the negative control, with normalized invasion/survival rates of 100%. Given values are means, with error bars representing 95% confidence intervals.

high-dose intravenous infection. If cytokine analysis had been possible at these later time points, elevated cytokine levels might have been observed in brain tissue. It is also possible that the lack of inflammatory response in the CNS may be a species-specific phenomenon and that guinea pigs or rabbits that display caseous necrosis in response to tuberculosis [25] may produce a more robust immunological response.

Because of the unique physiological barrier surrounding the CNS and the unique microenvironment in brain tissue, distinct from that in the lung, we hypothesized that certain bacterial genes may be specifically involved in invasion of the CNS from the systemic circulation as well as survival and growth within the CNS. Data from one clinical study also suggested different invasive abilities of *M. tuberculosis* strains with strain-specific compartmentalization in the lungs or the CNS [26]. *M. tuberculosis* genes *Rv0311, Rv0805, Rv0931c, Rv0986,* and *MT3280* were identified as having specific roles in invasion of and/or survival in the CNS, with no role identified in lung tissue. *Rv0986* is part of a 3-gene operon, *Rv0986–88,* absent in nonpathogenic mycobacteria [27] and is up-regulated during infection in an in vitro human BBB model [10]. *Rv0986–88* is predicted to form an ATP-binding cassette (ABC) transporter and is thought to be involved in cell adhesion and entry [28]. The *Rv0986* mutant has reduced capacity to bind to macrophages and invade endothelial cells, explaining its role during invasion observed in this study [10, 29]. *Rv0931c (pknD)* encodes a serine-threonine protein kinase (STPK) and is up-regulated in *M. tuberculosis* 24 and 96 h after in vitro nutrient starvation [30]. A recent study has shown that overexpression of *pknD* alters transcription of numerous downstream target genes, including *Rv0516c,* a putative anti–anti-sigma factor, and genes regulated by SigF. Furthermore, pknD phosphorylates Rv0516c, resulting in reduced binding of Rv0516c to the anti–anti-sigma factor Rv2638 [31]. Because STPK modulates intracellular events in response to external stimuli, disruption of *pknD* may prevent adaptive responses by *M. tuberculosis* in an unfavorable environment and lead to its demise. Another target of pknD, *Rv1747,* encoding a putative ABC transporter [32], is required for survival in an intravenous mouse model of infection [33]. Furthermore, Perez et al. have shown that pknD is involved in the phosphorylation of MmpL7, the transporter for phthiocerol dimycocerosate (PDIM), a lipid essential for virulence [34]. It is therefore intriguing to hypothesize that disruption of *pknD* may alter PDIM transport and therefore help reduce virulence. A possible explanation for the CNS-specific phenotype of pknD disruption may be the fact that pknD is positioned within a genomic regulon annotated as associated with phosphate regulation. The relatively low levels of inorganic phosphate within the brain (2.17 μmol/g) may contribute toward the attenuated phenotype observed in this study [36]. *Rv0805* encodes a cyclic nucleotide phosphodiesterase—the only such protein in *M. tuberculosis* [36]—whereas *Rv0311* and *MT3280* encode conserved hypothetical proteins. The mechanisms responsible for their role in the pathogenesis of CNS tuberculosis are also unclear and will be the focus of future studies.

The present study used a pooled mutant infection to assess the role played by *M. tuberculosis* genes in invasion of or survival in the CNS. This is potentially confounding, because defective mutants may be complemented by extracellular transactivating factors secreted by other mutants in the pool. However, none of the 5 genes identified in this study are predicted to encode extracellular factors. Furthermore, defective invasion or survival of all 5 mutants observed during single-mutant infections of the human in vitro CNS model may also support their role in CNS tubercu-

losis. Because brain and lung tissues are complex and are formed of several cell types, however, it is possible that defective invasion or survival of these mutants in other cell types not tested in this study also contributes to the phenotypes observed. Polar effects on downstream genes may also confound our results. For *Rv0986,* we do not anticipate polar effects on genes outside the *Rv0986–88* operon, because both the upstream gene, *mscL (Rv0985c),* and the downstream gene, *grcC2 (Rv0989c),* are oriented in the opposite direction. For similar reasons, polar effects on genes adjacent to *Rv0805, Rv0931c,* and *MT3280* are less likely. Polar effects on the downstream gene, *Rv0312,* may be responsible for the phenotype observed for *Rv0311*. Single-mutant infections in the in vivo model with these mutants and their complemented strains are under way to further characterize the role played by these genes in CNS tuberculosis. Finally, the present study did not evaluate the in vivo expression of the 5 identified *M. tuberculosis* genes during CNS infection with wild-type *M. tuberculosis*. Such an evaluation is challenging, because the infected whole mouse brain contains, at most, 1×10^4 bacilli. Although we have been able to quantify DNA from *M. tuberculosis* Tn mutants from so few bacteria because of amplification by prior growth on culture plates, this technique is obviously not suitable for studying RNA expression. Furthermore, because of contamination with eukaryotic RNA, it is logistically difficult to obtain sufficient quantities of bacterial RNA for analysis with such a low number of organisms. We are pursuing avenues to resolve these problems as part of another project looking at the gene expression profile of *M. tuberculosis* during CNS infection.

We have developed a method to identify *M. tuberculosis* genetic requirements for survival or invasion in the CNS. Intravenous administration of *M. tuberculosis* in this model simulates disseminated hematogenous tuberculosis, which is responsible for CNS tuberculosis and subsequent meningitis, as seen in humans. We have further demonstrated that, although lung tissue exhibits extensive inflammation and elevated cytokine levels, brain tissue lacks such an immune response for at least several weeks after infection. This observation is consistent with human data and may explain the paradoxical responses seen in human CNS tuberculosis. Using a pooled infection of genotypically defined mutants, we have shown specific genetic requirements for *M. tuberculosis,* distinct from lung tissue, for invasion of or survival in the CNS. Our screening method, along with characterization of the intravenously infected mouse model, will help in understanding the microbial and host processes involved in CNS invasion by *M. tuberculosis*. This may help in the development of better preventive strategies for this devastating disease.

Acknowledgment

We are grateful to Dr. Khairul-Bariah Abdul-Majid for her assistance with the cytokine analysis.

References

1. Thwaites G, Chau TT, Mai NT, Drobniewski F, McAdam K, Farrar J. Tuberculous meningitis. J Neurol Neurosurg Psychiatry **2000**; 68:289–99.
2. Hosoglu S, Geyik MF, Balik I, et al. Predictors of outcome in patients with tuberculous meningitis. Int J Tuberc Lung Dis **2002**; 6:64–70.
3. Berenguer J, Moreno S, Laguna F, et al. Tuberculous meningitis in patients infected with the human immunodeficiency virus. N Engl J Med **1992**; 326:668–72.
4. Katrak SM, Shembalkar PK, Bijwe SR, Bhandarkar LD. The clinical, radiological and pathological profile of tuberculous meningitis in patients with and without human immunodeficiency virus infection. J Neurol Sci **2000**; 181:118–26.
5. Thwaites GE, Hien TT. Tuberculous meningitis: many questions, too few answers. Lancet Neurol **2005**; 4:160–70.
6. Ransohoff RM, Kivisakk P, Kidd G. Three or more routes for leukocyte migration into the central nervous system. Nat Rev Immunol **2003**; 3: 569–81.
7. Rich AR, McCordock HA. The pathogenesis of tuberculous meningitis. Bull Johns Hopkins Hosp **1933**; 52:5–37.
8. Tsenova L, Ellison E, Harbacheuski R, et al. Virulence of selected *Mycobacterium tuberculosis* clinical isolates in the rabbit model of meningitis is dependent on phenolic glycolipid produced by the bacilli. J Infect Dis **2005**; 192:98–106.
9. van Well GTJ, Wieland CW, Florquin S, Roord JJ, van der Poll T, van Furth AM. A new murine model to study the pathogenesis of tuberculous meningitis. J Infect Dis **2007**; 195:694–7.
10. Jain SK, Paul-Satyaseela M, Lamichhane G, Kim KS, Bishai WR. *Mycobacterium tuberculosis* invasion and traversal across an in vitro human blood-brain barrier as a pathogenic mechanism for central nervous system tuberculosis. J Infect Dis **2006**; 193:1287–95.
11. Armand-DeLille PF. Role des poisons du bacille de Koch dans la meningite tuberculeuse et la tuberculose des centres nerveux; etude experimentale et anatomo-pathologique. Paris: Université de Paris, **1903**:187.
12. Donald PR, Schaaf HS, Schoeman JF. Tuberculous meningitis and miliary tuberculosis: the Rich focus revisited. J Infect **2005**; 50:193–5.
13. Tuberculosis Animal Research and Gene Evaluation Taskforce. Mutant collection. Available at: http://webhost.nts.jhu.edu/target/. Accessed 26 November 2007.
14. Jain SK, Hernandez-Abanto SM, Cheng QJ, et al. Accelerated detection of *Mycobacterium tuberculosis* genes essential for bacterial survival in guinea pigs, compared with mice. J Infect Dis **2007**; 195:1634–42.
15. Mitruka BM, Rawnsley HM. Clinical, biochemical and hematological reference values in normal experimental animals and normal humans. New York: Masson Publishing, **1981**.
16. Harkness JE, Wagner JE. The biology and medicine of rabbits and rodents. 3rd ed. Philadelphia: Lea & Febiger, **1989**.
17. Larsen M. Some common methods in mycobacterial genetics. In: Hatfull GF, Jacobs WR Jr, eds. Molecular genetics of mycobacteria. Washington, DC: ASM Press, **2000**:316–7.
18. Apostolakis S, Papadakis EG, Krambovitis E, Spandidos DA. Chemokines in vascular pathology (review). Int J Mol Med **2006**; 17:691–701.
19. Orme IM, Cooper AM. Cytokine/chemokine cascades in immunity to tuberculosis. Immunol Today **1999**; 20:307–12.
20. Galea I, Bechmann I, Perry VH. What is immune privilege (not)? Trends Immunol **2007**; 28:12–8.
21. Wu HS, Kolonoski P, Chang YY, Bermudez LE. Invasion of the brain and chronic central nervous system infection after systemic *Mycobacterium avium* complex infection in mice. Infect Immun **2000**; 68:2979–84.
22. Jain SK, Kwon P, Moss WJ. Management and outcomes of intracranial tuberculomas developing during antituberculous therapy: case report and review. Clin Pediatr (Phila) **2005**; 44:443–50.
23. Ford AL, Foulcher E, Lemckert FA, Sedgwick JD. Microglia induce CD4 T lymphocyte final effector function and death. J Exp Med **1996**; 184: 1737–45.

24. Matyszak MK, Perry VH. Bacillus Calmette-Guérin sequestered in the brain parenchyma escapes immune recognition. J Neuroimmunol **1998**; 82:73–80.
25. Flynn JL. Lessons from experimental *Mycobacterium tuberculosis* infections. Microbes Infect **2006**; 8:1179–88.
26. Garcia de Viedma D, Marin M, Andres S, Lorenzo G, Ruiz-Serrano MJ, Bouza E. Complex clonal features in an *Mycobacterium tuberculosis* infection in a two-year-old child. Pediatr Infect Dis J **2006**; 25:457–9.
27. Talaat AM, Lyons R, Howard ST, Johnston SA. The temporal expression profile of *Mycobacterium tuberculosis* infection in mice. Proc Natl Acad Sci USA **2004**; 101:4602–7.
28. Braibant M, Gilot P, Content J. The ATP binding cassette (ABC) transport systems of *Mycobacterium tuberculosis*. FEMS Microbiol Rev **2000**; 24:449–67.
29. Rosas-Magallanes V, Stadthagen-Gomez G, Rauzier J, et al. Signature-tagged transposon mutagenesis identifies novel *Mycobacterium tuberculosis* genes involved in the parasitism of human macrophages. Infect Immun **2007**; 75:504–7.
30. Betts JC, Lukey PT, Robb LC, McAdam RA, Duncan K. Evaluation of a nutrient starvation model of *Mycobacterium tuberculosis* persistence by gene and protein expression profiling. Mol Microbiol **2002**; 43:717–31.
31. Greenstein AE, MacGurn JA, Baer CE, Falick AM, Cox JS, Alber T. *M. tuberculosis* Ser/Thr protein kinase D phosphorylates an anti-anti–sigma factor homolog. PLoS Pathog **2007**; 3:e49.
32. Grundner C, Gay LM, Alber T. *Mycobacterium tuberculosis* serine/threonine kinases PknB, PknD, PknE, and PknF phosphorylate multiple FHA domains. Protein Sci **2005**; 14:1918–21.
33. Curry JM, Whalan R, Hunt DM, et al. An ABC transporter containing a forkhead-associated domain interacts with a serine-threonine protein kinase and is required for growth of *Mycobacterium tuberculosis* in mice. Infect Immun **2005**; 73:4471–7.
34. Perez J, Garcia R, Bach H, et al. *Mycobacterium tuberculosis* transporter MmpL7 is a potential substrate for kinase PknD. Biochem Biophys Res Commun **2006**; 348:6–12.
35. Hawkins RA, Nielsen RC, Veech RL. The measurement of the inorganic phosphate content of brain in the presence of bone fragments. J Neurochem **1973**; 20:35–38.
36. Shenoy AR, Capuder M, Draskovic P, Lamba D, Visweswariah SS, Podobnik M. Structural and biochemical analysis of the Rv0805 cyclic nucleotide phosphodiesterase from *Mycobacterium tuberculosis*. J Mol Biol **2007**; 365:211–25.